

Theoretical understanding of the quasiparticle dispersion in bilayer high- T_c superconductors

Jian-Xin Li^{1,2,3}, T. Zhou¹, and Z. D. Wang^{1,2}

¹*National Laboratory of Solid State Microstructures and Department of Physics, Nanjing University, Nanjing 210093, China*

²*Department of Physics, The University of Hong Kong, Pokfulam Road, Hong Kong, China*

³*The Interdisciplinary Center of Theoretical Studies, Chinese Academy of Sciences, Beijing, China.*

(Dated: November 12, 2018)

The renormalization of quasiparticle (QP) dispersion in bilayer high- T_c cuprates is investigated theoretically by examining respectively the interactions of the QP with spin fluctuations (SF) and phonons. It is illustrated that both interactions are able to give rise to a kink in the dispersion around the antinodes (near $(\pi, 0)$). However, remarkable differences between the two cases are found for the peak/dip/hump structure in the lineshape, the QP weight, and the interlayer coupling effect on the kink, which are suggested to serve as a discriminant to single out the dominant interaction in the superconducting state. A comparison to recent photoemission experiments shows clearly that the coupling to the spin resonance is dominant for the QP around antinodes in bilayer systems.

PACS numbers:

The elucidation of many-body interactions in high- T_c superconductors (HTSC) is considered as an essential step toward an insightful understanding of their superconductivity. Angle-resolved photoemission spectroscopy (ARPES) has provided a powerful way to probe the coupling of charge QPs to other QPs or collective modes. Recent ARPES experiments unveil several intriguing features in the dispersion, the QP weight, and the lineshape: (i) A kink in the dispersion was observed in both the nodal and antinodal regions [1, 2, 3, 4]. (ii) The QP weight around the antinodal region decreases rapidly with the reduction of dopings [5], while changes a little around the nodal direction [6]. (iii) After disentangling the bilayer splitting effect, an intrinsic peak/dip/hump (PDH) structure was seen around the antinodal region both in the bonding (BB) and antibonding (AB) band [2, 3]. (iv) The kink around the antinodal region seems to show a different momentum, temperature and doping dependence from that around the nodal direction [2]. (v) The antinodal kink is likely absent (or very weak) in the single-layered Bi2201 [4]. These features, especially (i), imply that the QP is coupled to a collective mode. So far, two collective modes of 41 meV spin resonance [7, 8] and ~ 36 meV phonon [9, 10] have been suggested, but which one is a key factor responsible for the kink is still much debatable [1, 2, 3, 4, 9, 10, 11]. So, it raises an important question as if the electronic interaction alone is responsible for the intriguing QP dispersion, or to what extent the antinodal (nodal) QP's properties are determined by the strong electronic interaction.

In this Letter, we not only answer the above important question but also present a coherent understanding on the above features by studying in detail the respective effects of the fermion-SF interaction and fermion-phonon interaction on the QP dispersion based on the slave-boson theory of the bilayer $t-t'-J$ model. We find that though both couplings are able to give rise to the kink structure near the antinodal region in the QP dispersion,

they differ remarkably in the following aspects. (a) The lineshape arising from the spin resonance coupling exhibits a clear PDH structure, while the phonon coupling would lead to a reversed PDH structure, namely the peak is in a larger binding energy than the hump. (b) The former coupling causes a rapid drop of the QP weight near the antinodal region with underdoping, but the latter has only a very weak effect. Moreover, the corresponding coupling constant for the fermion-SF interaction is reasonable consistent with ARPES data, in contrast to the much smaller value for the fermion-phonon interaction. (c) The bilayer coupling plays a positive role in the occurrence of the kink in the case of the fermion-SF interaction, but has a negative effect on the formation of the kink for the fermion-phonon interaction. These results suggest that the SF coupling be a dominant interaction involved in the antinode-to-antinode scattering.

We will consider separately the interactions of fermions with the SF and phonons. Let us start with the bilayer $t-t'-J$ model with the AF interaction included,

$$H = - \sum_{\langle ij \rangle, \alpha, \alpha', \sigma} t_{\alpha, \alpha'} c_{i\sigma}^{(\alpha)\dagger} c_{j\sigma}^{(\alpha')} - \sum_{\langle ij \rangle', \alpha, \sigma} t' c_{i\sigma}^{(\alpha)\dagger} c_{j\sigma}^{(\alpha)} - h.c. + \sum_{\langle ij \rangle, \alpha, \alpha'} J_{\alpha, \alpha'} \mathbf{S}_i^{(\alpha)} \cdot \mathbf{S}_j^{(\alpha')}, \quad (1)$$

where $\alpha = 1, 2$ denotes the layer index, $t_{\alpha, \alpha'} = t$, $J_{\alpha, \alpha'} = J$ if $\alpha = \alpha'$, otherwise, $t_{\alpha, \alpha'} = t_p/2$, $J_{\alpha, \alpha'} = J_{\perp}/2$ and $i = j$. Other symbols are standard. In the slave-boson representation, the electron operators $c_{j\sigma}$ are written as $c_{j\sigma} = b_j^\dagger f_{j\sigma}$, where fermions $f_{i\sigma}$ carry spin and bosons b_i represent the charge. Using the mean field parameters $\chi_{ij} = \sum_{\sigma} \langle f_{i\sigma}^\dagger f_{j\sigma} \rangle = \chi_0$, $\Delta_{ij} = \langle f_{i\uparrow} f_{j\downarrow} - f_{i\downarrow} f_{j\uparrow} \rangle = \pm \Delta_0$, and setting $b \rightarrow \sqrt{\delta}$ with δ the doping density (boson condense), we can decouple the Hamiltonian (1). Its Fourier transformation is given by, $H_m = \sum_{\mathbf{k}\sigma\alpha} \varepsilon_{\mathbf{k}\sigma\alpha} f_{\mathbf{k}\sigma}^{(\alpha)\dagger} f_{\mathbf{k}\sigma}^{(\alpha)} - \sum_{\mathbf{k}\alpha} \Delta_{\mathbf{k}} (f_{\mathbf{k}\uparrow}^{(\alpha)\dagger} f_{-\mathbf{k}\downarrow}^{(\alpha)} + h.c.) + \sum_{\mathbf{k}\sigma} [\delta t_{\perp} e^{ik_z c} f_{\mathbf{k}\sigma}^{(1)\dagger} f_{\mathbf{k}\sigma}^{(2)} + h.c.] + \varepsilon_0$, with $\varepsilon_{\mathbf{k}} =$

$-2(\delta t + J'\chi_0)(\cos k_x + \cos k_y) - 4\delta t' \cos k_x \cos k_y - \mu_f$, $\Delta_k = 2J'\Delta_0(\cos k_x - \cos k_y)$, $\varepsilon_0 = 4NJ'(\chi_0^2 + \Delta_0^2)$, $t_{\perp\mathbf{k}} = t_p(\cos k_x - \cos k_y)^2/4$ [12] and $J' = 3J/8$. Diagonalizing the Hamiltonian, we get the AB and BB bands with the dispersion $\epsilon^{(A,B)} = \varepsilon_{\mathbf{k}} \pm \delta t_{\perp\mathbf{k}}$. Then, the bare normal (abnormal) Green's functions of fermions $\mathcal{G}_s^{(A,B)}$ ($\mathcal{G}_w^{(A,B)}$), and the bare spin susceptibility $\chi^{\alpha,\alpha'}(\alpha, \alpha' = A, B)$ are obtained. The physical spin susceptibility is given by $\chi = \chi_0^+ \cos^2(q_z c/2) + \chi_0^- \sin^2(q_z c/2)$, with $\chi_0^+ = \chi^{AA} + \chi^{BB}$ and $\chi_0^- = \chi^{AB} + \chi^{BA}$.

The slave-boson mean-field theory underestimates the AF correlation [13, 14], so we need to go beyond it and include the effect of SF through the random-phase approximation (RPA), in which the renormalized spin susceptibility is,

$$\chi^{\pm}(\mathbf{q}, \omega) = \chi_0^{\pm}(\mathbf{q}, \omega) / [1 + (\alpha J_{\mathbf{q}} \pm J_{\perp}) \chi_0^{\pm}(\mathbf{q}, \omega) / 2] \quad (2)$$

However, in the ordinary RPA ($\alpha = 1$), the AF correlation is overestimated as indicated by a larger critical doping density $\delta \approx 0.22$ for the AF instability than the experimental data $\delta_c = 0.2 \sim 0.5$ [15]. Thus, we use the renormalized RPA in which the parameter α is determined by setting the AF instability at the experimental value δ_c . The fermionic self-energy coming from the SF coupling is given by,

$$\Sigma_{s,w}^{(A,B)}(\mathbf{k}) = \pm \frac{1}{4N\beta} \sum_{\mathbf{q}} [(J_{\mathbf{q}} + J_{\perp})^2 \chi^+(\mathbf{q}) \mathcal{G}_{s,w}^{(A,B)}(\mathbf{k} - \mathbf{q}) + (J_{\mathbf{q}} - J_{\perp})^2 \chi^-(\mathbf{q}) \mathcal{G}_{s,w}^{(B,A)}(\mathbf{k} - \mathbf{q})], \quad (3)$$

where, the $+$ ($-$) sign is for the normal (abnormal) self-energy $\Sigma_{s(w)}$, and the symbol \mathbf{q} represents an abbreviation of $\mathbf{q}, i\omega_m$. The renormalized Green's function is $G^{(A,B)}(\mathbf{k}, i\omega) = [(G_s^{(A,B)}(\mathbf{k}, i\omega))^{-1} + (\Delta_{\mathbf{k}} + \Sigma_w^{(A,B)})^2 G_s^{(A,B)}(\mathbf{k}, -i\omega)]^{-1}$ with $G_s^{(A,B)} = [i\omega - \epsilon^{(A,B)} - \Sigma_s^{(A,B)}]^{-1}$, and the spectral function is obtained via $A(k, \omega) = -(1/\pi) \text{Im}[G(k, \omega + i\delta)]$. To determine the QP weight z , we first write the Green's function as $G(\mathbf{k}, i\omega) = M/(i\omega + \Sigma_{\alpha}) + N/(i\omega - \Sigma_{\beta})$ and get z via $z = M/[1 + \partial \Sigma_{\alpha} / \partial \omega(\omega_0)]$, with ω_0 the pole of G . The parameters we choose are $t = 2J$, $t' = -0.7t$, $J = 120$ meV and $J_{\perp} = 0.1J$ [15]. Except in Fig.4, the doping density is set at $\delta = 0.2$.

Fig.1 (a) and (b) display the calculated QP dispersion for the BB band obtained from the momentum distribution curve (MDC) [16] in the antinodal and nodal regions, respectively. One can see from Fig.1(a) that the antinodal kink appears in some range of parameters t_p and α , such as $t_p = 2.0J$ and $\alpha = 0.43$. The RPA correction factor $\alpha = 0.34, 0.43$ and 0.55 correspond to the critical doping density of the AF instability $\delta_c = 0.02, 0.05$ and 0.09 , while $\delta_c = 0.02 \sim 0.05$ is within the experimental range [15]. Meanwhile, the ARPES experiment indicated that $t_{\perp, \text{exp}}$ (corresponding to δt_p , $\delta \sim 0.2$) is 44 ± 5 meV [17], i.e., $t_p = 1.6 \sim 2.0J$ here. Therefore, in the reasonable parameter range, the interaction between fermions and SF reproduces well the observed antinodal

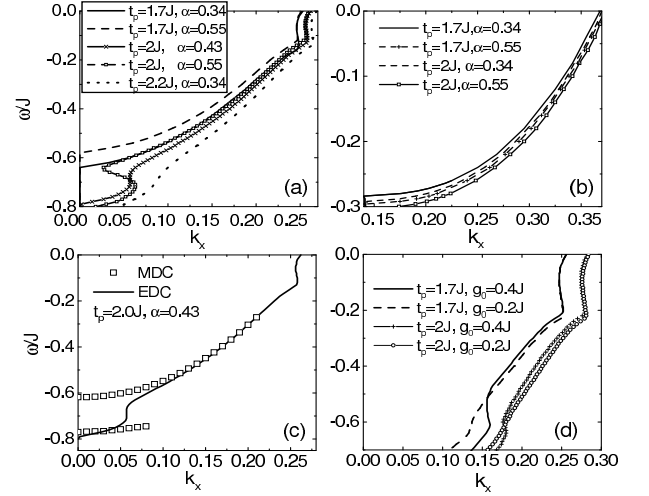


FIG. 1: The MDC dispersion of fermions due to the interaction with spin fluctuations (a),(b) and (c), and phonons (d). Figs.(a),(c) and (d) are the results at (k_x, π) (antinodal region), and Fig.(b) at (k_x, k_x) (nodal direction). The scattered points in Fig.(c) are derived from the EDC [16].

kink. In contrast, Fig.1(b) shows that no kink is present in the nodal region. This can be understood from the conservation of the momentum in the scattering process, namely the nodal-to-nodal scattering involves a smaller transferred momentum than $\mathbf{Q} = (\pi, \pi)$ where the AF spin fluctuation peaks. Thus, we will focus mainly on the antinodal region in the following discussion. In Fig.1(c) we replot the MDC dispersion together with the EDC derived dispersion [16]. Near and below the region where the kink appears in the MDC dispersion, the EDC dispersion breaks into a two-part structure, a peak and a hump. Therefore, the appearance of the antinodal kink has an intimate relation to the PDH structure in the EDC plot, being in agreement with experiments [18].

In fact, the kink may also be expected if fermions are predominantly coupled to other collective modes. A hotly discussed mode responsible for the antinodal kink is the out-of-plane out-of-phase O bucking B_{1g} phonon [9, 10]. To take into account this kind of mode, we may have the total Hamiltonian by including the following interaction in the slave-boson mean field Hamiltonian H_m ,

$$H_{ep} = \frac{1}{\sqrt{N}} \sum_{\mathbf{k}, \mathbf{q}, \sigma} g(\mathbf{k}, \mathbf{q}) f_{\mathbf{k}, \sigma}^{\dagger} f_{\mathbf{k}+\mathbf{q}, \sigma} (d_{\mathbf{q}}^{\dagger} + d_{-\mathbf{q}}) \quad (4)$$

where d^{\dagger} and d are the creation and annihilation operators for phonons, $g(\mathbf{k}, \mathbf{q}) = g_0 [\Phi_x(\mathbf{k}) \Phi_x(\mathbf{k} - \mathbf{q}) \cos(q_y/2) - \Phi_y(\mathbf{k}) \Phi_y(\mathbf{k} - \mathbf{q}) \cos(q_x/2)] / \sqrt{\cos^2 q_x/2 + \cos^2 q_y/2}$ and the detailed form of Φ_x, Φ_y can be found in Ref. [9, 10]. We note that the vertex $g(\mathbf{k}, \mathbf{q} = 0) \sim \cos(k_x) - \cos(k_y)$ and vanishes for all \mathbf{k} at $\mathbf{q} = (\pi, \pi)$ [9, 10]. Thus, the fermions near $(\pi, 0)$ are strongly scattered by this interaction. The corresponding fermionic self-energy is given

by,

$$\Sigma_{s,w}(\mathbf{k}) = \pm \frac{1}{\beta N} \sum_{\mathbf{q}} |g(\mathbf{k} - \mathbf{q}, \mathbf{q})|^2 D_0(\mathbf{q}) [\mathcal{G}_{s,w}^{(A)}(\mathbf{k} - \mathbf{q}) + \mathcal{G}_{s,w}^{(B)}(\mathbf{k} - \mathbf{q})]. \quad (5)$$

where the Green's function of phonon is $D_0(\mathbf{q}) = 2\omega_q / [(i\omega)^2 - (\omega_q)^2]$, and a dispersionless optical phonon (B_{1g}) will be taken as $\hbar\omega_q = 36\text{meV}$ [9, 10]. Unlike the fermion-SF interaction, the coupling constant here is not available now. We have tried various values and found that the well-established kink can be obtained when $g_0 \approx 0.2J \sim 0.4J$ if $t_p = 1.7J$ as shown in Fig.1(d). This result is quite similar to that for the SF in Fig.1(a). So, a mere reproduction of the QP kink is not sufficient to single out the main cause of the renormalization, and we must resort to other features.

A meaningful difference between the effects of these two interactions on the dispersion can be seen clearly from a comparison of Fig.1(a) and (d), namely, the inter-layer coupling t_p has opposite impacts on the antinodal kink. It enhances the kink feature for the fermion-SF interaction; as shown in Fig.1(a), when t_p decreases to $1.7J$, no antinodal kink is observed even for the strongest AF coupling $\alpha = 0.55$ which is in fact beyond the experimentally acceptable value. In contrast, the kink feature is weakened by the interlayer coupling for the fermion-phonon interaction; as seen in Fig.1(d), the kink disappears when t_p increases to $2J$ from $1.7J$ with $g_0 = 0.2J$. Recent ARPES experiments revealed that a more pronounced kink is present in the multilayered BiSrCaCuO, in sharp contrast to the case in the single-layered one [4], which can be considered as an indication to favor the fermion-SF interaction in the bilayer system. Because the spin susceptibility in the bilayer system involves scatterings between layers, the self-energy [Eq.(3)] has a feature that the fermions in the BB (AB) band is scattered into AB (BB) band via the SF in the odd channel χ^- . The so-called spin resonance (a sharp peak in $\text{Im}\chi$) appears around \mathbf{Q} both in the odd χ^- and even χ^+ channels (see Fig.2(a)). However, it is more prominent in the odd channel, which is in agreement with very recent experiments [19], mainly due to the larger vertex $\alpha J_{\mathbf{Q}} - J_{\perp}$ ($J_{\mathbf{Q}} = -2J$) [Eq.(2)], compared to $\alpha J_{\mathbf{Q}} + J_{\perp}$ in the even channel. On the other hand, the AB band (and its associated flat band near \mathbf{Q}) is much close to the Fermi surface compared to the BB band, as shown in Fig.2(b). As a result, the fermionic self-energy for BB band is large, and consequently the renormalization is strong. We have indeed observed that the AB band is much less affected by this coupling, so no kink is present in this band (not shown here). As increasing t_p , the splitting between the AB and BB band pushes the flat portion of the AB band to be more close to the Fermi level [Fig.2(b) and (c)], so enhances the scattering [20]. However, for the coupling to phonons, the AB and BB bands contribute to the self-energy in the same way [Eq.(5)]. In this case, though the increase of t_p increases the contribution from the AB

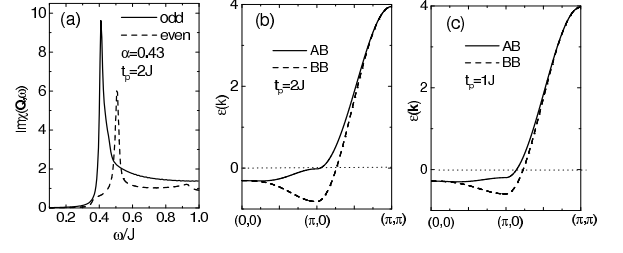


FIG. 2: (a) $\text{Im}\chi(\mathbf{q}, \omega)$ vs ω at (π, π) . (b) and (c) show the bare dispersion of the normal state quasiparticle for $t_p = 2J$ and $1.0J$, respectively.

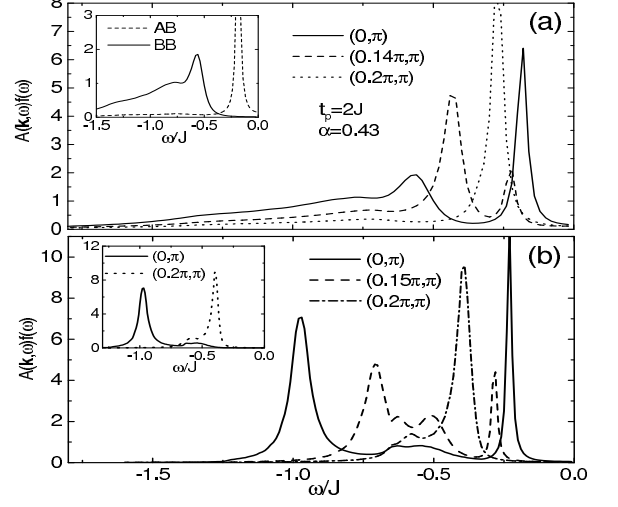


FIG. 3: The lineshape of fermions at different k points. Fig.(a) is obtained when fermions is coupled to spin fluctuations. Fig.(b) shows the result arising from the coupling to the B_{1g} phonons. The inset in Fig.(a) shows the lineshape for the bonding and antibonding bands at $(0, \pi)$, separately. The inset in Fig.(b) is the lineshape for the bonding band at $k = (0, \pi)$ and $(0.2\pi, \pi)$.

band, the decrease from the BB band overcompensates that increase, and thus the self-energy decreases with t_p on the whole.

In Fig.3, we show the lineshape for different k points from $(0, \pi)$ to $(0, 0.2\pi)$. For the fermion-SF interaction, both the BB and AB spectra near $(0, \pi)$ consist of a low energy peak, followed by a hump, and then a dip in between, though the intensity of the AB hump is much weaker than its peak intensity [inset of Fig.3(a)]; both develop their own PDH structure near $(0, \pi)$. When moving from $(0, \pi)$ to $(0.2\pi, \pi)$, one will see that the intensity of the BB peak increases, while the AB peak decreases rapidly. Eventually, only the BB peak can be seen near $(0.2\pi, \pi)$. These features are in good agreement with ARPES experiments [17]. However, the lineshape caused by the phonon-coupling displays a striking contrast to those shown in Fig.3(a) and in experiments [17], namely, the peak is far below the dip and the dip is below the hump [Fig.3(b)]. This is because the renor-

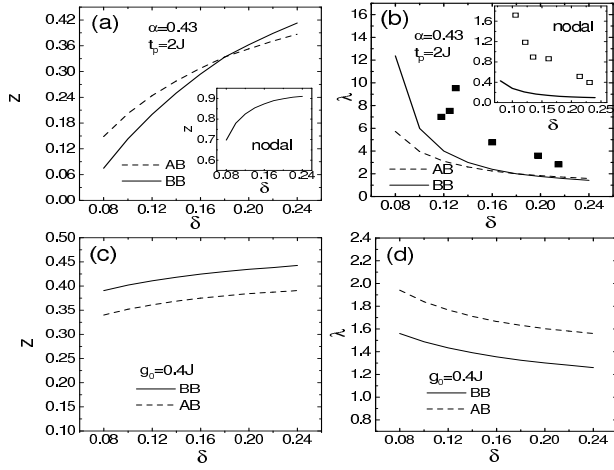


FIG. 4: The quasiparticle weight z of fermions and its coupling constant λ at the antinodes arising from the coupling to spin fluctuations (a) and (b), and to phonons (c) and (d). The insets show those at the nodes. The scattered points are experimental data from Ref. [3] and Ref. [6].

malization to the QP peak in the BB band due to the phonons is rather weak, so the peak is almost unchanged comparing to the bare one. When moving from $(0, \pi)$ to $(0.2\pi, \pi)$, the QP moves to be near the Fermi level, an ordinary PDH structure is recovered [inset of Fig.3(b)] because the hump arising from the phonon coupling does not change in the process.

Figure 4 presents the QP weight z of fermions and the coupling constant λ . Notice that the weight of the physical electron is δz due to the condensation of holons in the slave-boson approach [13]. For the fermion-SF interaction, the weight decreases rapidly with underdoping, from nearly 0.42 and 0.39 at doping $\delta = 0.24$ (the bare value is 0.5) to be below 0.075 and 0.15 at $\delta = 0.08$ for the BB and AB band, respectively. On the other hand, the weight along the nodal direction decreases very

slowly, and it is still 0.7 even at $\delta = 0.08$. This exhibits the highly anisotropic interaction between fermions and SF and is well consistent with what is inferred from ARPES [5] and a recent argument based on the analysis of experimental data [21]. Moreover, the coupling constant obtained using $z = 1/(1 + \lambda)$ shows a reasonable fit to experimental data [3][Fig.4(b)], while that at the nodal direction is much smaller than the experimental data [6] [inset of Fig.4(b)]. This consistence is significant, because we use the well established parameters in the $t - t' - J$ model with only one adjustable parameter α being fixed by fitting to experiments. In contrast, the weight decreases much slowly for the fermion-phonon interaction as shown in Fig.4(c), and the coupling constant λ is nearly 3 ~ 5 times smaller than experimental values.

Finally, we wish to make two additional remarks. First, because the spin resonance contributes little to the node-to-node scattering, a kink structure in the nodal direction should be caused by the other mode coupling, such as an in-plane Cu-O breathing phonon [1]. The different momentum, temperature and doping dependence between the nodal and antinodal kink [feature (iv)] supports this point of view. Second, since the interlayer coupling plays opposite roles in the antinodal kink respectively for the fermion-SF and fermion-phonon interactions, it is expected that, even though a rather weak fermion-phonon coupling may be present and lead to a weak antinodal kink-like behavior in the single-layered cuprates, as possibly seen in the experiment for Bi2201 [4], the coupling is too weak to affect significantly the lineshape which is mainly determined by the SF and was shown to exhibit the peak/dip/hump structure in the single-layered case [14].

We are grateful to F.C. Zhang for many useful discussions. The work was supported by the NSFC (10474032, 10021001, 10429401, 10334090), the RGC of Hong Kong (HKU 7050/03P), the URC fund of HKU, and partly by RFDP (20030284008).

-
- [1] A. Lanzara *et al.*, Nature **412**, 510 (2001).
 - [2] S. V. Borisenko *et al.*, Phys. Rev. Lett. **90**, 207001 (2003); A. D. Gromko *et al.*, Phys. Rev. B **68**, 174520 (2003).
 - [3] T.K. Kim *et al.*, Phys. Rev. Lett. **91**, 167002 (2003).
 - [4] T. Sato *et al.*, Phys. Rev. Lett. **91**, 157003 (2003).
 - [5] A. Damascelli, Z. Hussain and Z. X. Shen, Rev. Mod. Phys. **75**, 473 (2003).
 - [6] P. D. Johnson *et al.*, Phys. Rev. Lett. **87**, 177007 (2001).
 - [7] H. F. Fong *et al.*, Phys. Rev. Lett. **75**, 316 (1995).
 - [8] P. Bourges *et al.*, Science **288**, 1234 (2000).
 - [9] T. Cuk *et al.*, Phys. Rev. Lett. **93**, 117003 (2004).
 - [10] T. P. Devereaux, T. Cuk, Z. X. Shen, and N. Nagaosa, Phys. Rev. Lett. **93**, 117004 (2004).
 - [11] M. Eschrig and M. R. Norman, Phys. Rev. Lett. **89**, 277005 (2002).
 - [12] O. K. Anderson *et al.*, J. Phys. Chem. Solids **56**, 1573 (1995).
 - [13] P. A. Lee, Physica C **317-318**, 194 (1999); J. Brinckmann and P.A. Lee, Phys. Rev. Lett. **82**, 2915 (1999).
 - [14] J. X. Li, C. Y. Mou, and T. K. Lee, Phys. Rev. B **62**, 640 (2000).
 - [15] A. P. Kampf, Phys. Rep. **249**, 219 (1994).
 - [16] Besides MDC, another intensity plot in ARPES is the energy distribution curve (EDC). Due to the abnormal lineshape of EDC [5], MDC is more often used to analyze the dispersion.
 - [17] D. L. Feng *et al.*, Phys. Rev. Lett. **86**, 5550 (2001).
 - [18] M. R. Norman *et al.*, Phys. Rev. B **64**, 184508 (2001).
 - [19] S. Pailhes *et al.*, cond-mat/0308394 (2003).
 - [20] Notice that the interlayer AF coupling J_{\perp} also enhances the coupling to spin resonance [see Eq.(3)].
 - [21] D. E. Sheehy, T. P. Davis, and M. Franz, cond-mat/0312529 (2003).